Electronic Supplementary Material (ESI) for Dalton Transactions.
This journal is © The Royal Society of Chemistry 2022

Supporting Information

for

Improving synthetic H_2 production catalyst design strategy with neurotransmitter dopamine

Santanu Ghorai,[a] Shikha Khandelwal,[b] Srewashi Das,[a] Surabhi Rai,[a,c] Somnath Guria,[a] Piyali Majumder,[c] and Arnab Dutta*[a, c, d]

[a]Chemistry Department, Indian Institute of Technology Bombay, Powai, Mumbai, India 400076

[b]Chemistry Discipline, Indian Institute of Technology Gandhinagar, Palaj, India 382355

[c]National Centre of Excellence in CCU, Indian Institute of Technology Bombay, Powai, Mumbai, India 400076.

[d]Interdisciplinary Program in Climate Studies, Indian Institute of Technology Bombay, Powai, Mumbai, India 400076

**Corresponding author: arnab.dutta@iitb.ac.in*

Table of contents

Experimental Section

Materials and Methods:

All the chemicals, solvents (Avra chemicals, Sigma Aldrich chemicals, and Finar chemicals) need no further purification. Cleaned and dried glass wares were used. Under an N_2 atmosphere Reactions were executed with the help of the schlenk-line technique. NMR spectra were recorded with the help of Bruker Avance II Ascent FT spectrometer (400 MHz) and Bruker Avance II Ascent FT spectrometer (500 MHz) for ^1H. Additionally, NMR solutions were reported in ppm with solutions in dmso-d^6 (d~2.5ppm). UV-VIS spectrua were recorded in 2 mL Sterna make quartz cuvette having 1 cm pathlength with the help of PerkinElmer Lambda 1050 spectrometers. FTIR spectra of solid samples were studied using KBr pellet on PerkinElmer (Spectrum-I) spectrometer. For determining the mass, HRMS of the samples were determined on Bruker Maxis impact in positive mode. At room temperature cyclic voltammetry (CV) experiments were recorded using Metrohm Autolab PGSTAT 204 potentiostat.

Electrochemical Studies:

All experimental CVs were studied in dry DMF or in an aqueous buffer medium using 0.1M MES hydrate in Millipore water with a solute concentration in the presence of anhydrous sodium sulphate as a supporting electrolyte. A standard three-electrode system of 1 mm glassy carbon disc as working electrode, Ag/AgCl as a reference electrode connected by Vycor tip, and platinum wire as counter electrode were used as the counter electrode. All potentials are reported versus Fc/Fc^+ for organic medium and $[Fe(CN)6]^{3-/4-}$ couple for aqueous medium E^0 $[Fe(CN)6]^{3-/4-}$= +0.360 V vs. SHE. The system was further connected to Metrohm Autolab PGSTAT 204 using 3 mm glassy carbon rod as a working electrode, Pt wire as a counter electrode, and Ag as a reference electrode with continuous Ar flow. The pH of the aqueous solutions was measured with the help of bench top Labman LMPH-10 pH Meter. For bulk electrolysis setup, a customized four-neck glass vessel (77 mL with headspace), coiled 23 cm Pt wire as a counter electrode, Ag rod as a reference electrode, and plastic carbon chip (1 cm x 2 cm) as working electrode were utilized.[1]

The last neck was closed by a B-14/20 suba seal rubber septum and used for N_2 purging before the experiment and for headspace gas collection for GC measurements. During the experiment, 14 mL of 0.1-0.25 mM complexes were added in the vessel, all electrodes (along with a magnetic bead) were inserted along with a B-14/20 rubber septum cap (gas tight), and

the solution was purged with N_2 for 30 minutes. Purging was stopped, and a chrono-coulometric experiment was started at corresponding catalytic potentials. Solution was stirred continuously with a magnetic stirrer during the experiment. Gastight PTFE leur lock 1000 series (1001TLL) 1 mL Hamiltonian syringe was used for collecting headspace gas after 1 hour of experiment. It was analyzed via gas chromatography (GC) instrument on TCD/FID mode. Headspace H_2 was detected by using Dhruva CIC gas chromatography (GC) with TCD/FID detector with a 5A^o molecular sieve/Porapak at room temperature. The instrument was calibrated manually by using different amounts of a control gas mixture containing 0.5% H_2, CH_4, N_2, and O_2.

The SEM-EDS study was done with the help of JEOL JSM7600F instrument at accelerating voltage of 5 kV. Energy-dispersive X-ray spectroscopy (EDS) was done with FE-SEM to trace the elemental composition.

Photocatalytic studies:

C1-C4 were taken in 10 ml pH 7.0 buffer solution in a test tube, followed by the addition of photosensitizer (EOSIN-Y) and 1 mL triethanolamine (TEOA) as a sacrificial electron donor. The concentration of the complexes in the solution is 0.1mM, and the concentration of the photosensitizer in each solution mixture is 0.2mM. The total volume of the reaction solution is 11mL. For photocatalytic illumination of the sample, Thor lab instrument (SLS301) with 350 -2700nm with 350-610nm bandpass filter used for filtering visible light required Eosin-Y PS. For all experiments, the beam size(3.80cm^2) and laser-power (40 mW/cm^2) were constant. Before starting the photo irradiation, each sample was degassed using Argon gas for 5 minutes. At 1 hour 0.5mL of gas was taken from the headspace, and examined the components of gas were through GC.

Calculation of catalytic rate:

The rate was calculated using the following equation:

$$\frac{i_c}{i_p} = \frac{n}{0.4463}\left(\frac{RTK_{obs}}{F\nu}\right)^{1/2} \quad \text{.....} \quad \textbf{(Equation S1)}$$

i_c= catalytic current, i_p=stoichiometric current, n= number of electrons transferred, F= Faraday Constant, R= Universal gas constant, T = temperature, K_{obs}=observed rate, ν= scan

rate.

Calculation of TON:

$$\textbf{TON} = \frac{No.\ of\ moles\ of\ H2\ produced}{No.\ of\ moles\ of\ catalyst\ used}$$

Calculation of Faradaic efficiency and TON of Complexes:

Current Efficiency of C3 at pH 7.0:

The overall charge passed during the catalytic HER= 5.32 C

The theoretical amount of Hydrogen expected = 5.32 C/(96485 × 2C) mol=27.55 micro moles

Experimentally H_2 detected in headspace by GC= 26.45 micromoles

Faradaic efficiency of **C3**=26.45/27.55 = 95.34%

Amount of **C3** in the solution= 1.0 micromoles

TON= (26.45/1.0)=26.45

Current Efficiency of C4 at pH 7.0:

The overall charge passed during the catalytic HER= 12.06 C

The theoretical amount of Hydrogen expected = 12.06 C/(96485 × 2C) mol=62.41 micro moles

Experimentally H_2 detected in headspace by GC= 41.53 micro moles

Faradaic efficiency of **C4** = 41.53/62.41=66.54%

Amount of **C4** in the solution= 2.5 micromoles

TON= (41.53/2.5)=16.61

Current Efficiency of C3 at pH 6.0:

The overall charge passed during the catalytic HER= 22.34 C

The theoretical amount of Hydrogen expected = 22.34 C/ (96485 × 2C) mol= 116.0 micro

moles

Experimentally H_2 detected in headspace by GC= 104.2 micro moles

Faradaic efficiency of **C3**= 104.2/116.0=89.82%

Amount of **C3** in the solution= 0.83 micromoles

TON= (104.2/0.83)=125

Current Efficiency of C4 at pH 6.0:

The overall charge passed during the catalytic HER= 23.55 C

The theoretical amount of Hydrogen expected = 23.55 C/ (96485 × 2C) mol= 122.3 micro moles

Experimentally H_2 detected in headspace by GC= 110.4 micro moles

Faradaic efficiency of **C4**= 110.4/122.3=90.27%

Amount of **C4** in the solution= 1.2 micromoles

TON= (110.4/1.2)=92

Current Efficiency of C4 at pH5:

The overall charge passed during the catalytic HER= 4.4 C

The theoretical amount of Hydrogen expected = 4.4 C/ (96485 × 2C) mol= 22.84 micro moles

Experimentally H_2 detected in headspace by GC= 20.54 micromoles

Faradaic efficiency of **C4**=20.54/22.84 = 90%

Amount of **C4** in the solution= 0.83 micromoles

TON= (20.54/0.83)=24.75

Current Efficiency of C2 at pH7:

The overall charge passed during the catalytic HER=7.96 C

The theoretical amount of Hydrogen expected=7.96 C/ (96485 × 2C) mol=41.25 micro moles

Experimentally H_2 detected in headspace by GC= 30.63 micro moles

Faradaic efficiency of **C2**= 30.63/41.25= 74%

Amount of **C2** in the solution= 3.5 micromoles

TON= (30.63/3.5)=8.77

Synthetic Procedure:

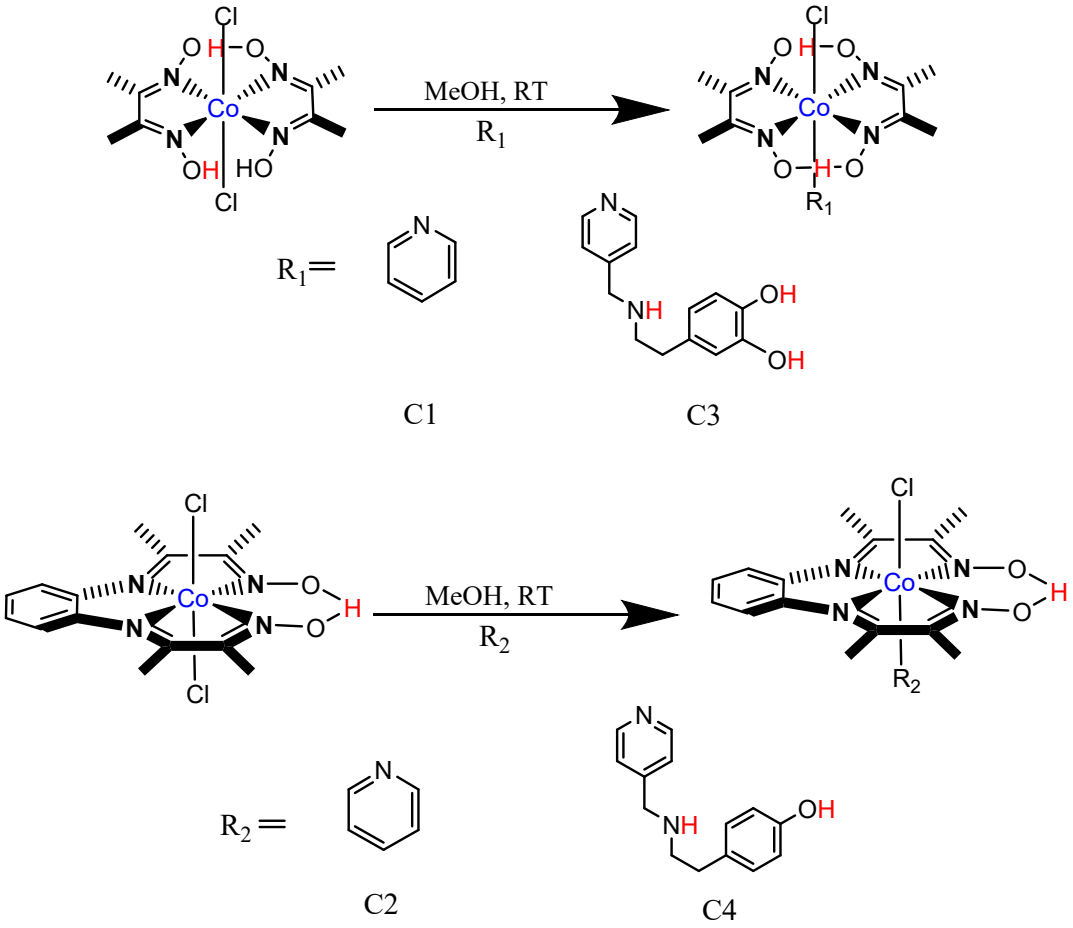

Scheme S1. Synthetic procedure for obtaining complexes **C1-C4**.

1.2.1. Synthesis of Copdd core (L1):

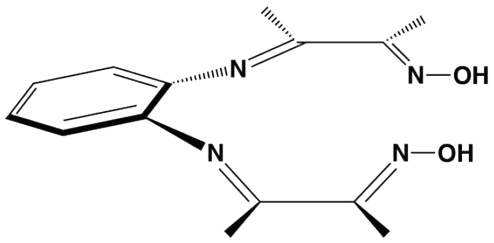

O-phenylenediamine (0.009 mol) was dissolved in 30 ml hot distilled water with continuous stirring. When *o*-phenylenediamine got dissolved completely, then diacetyl monoxime (0.018 mol) was added into it with constant stirring. It was allowed to reflux this dark yellow liquid for about 5 hours first, cooled the liquid at room temperature and then on an ice bath for 2 hours. The yellow product precipitated out of the solution. This precipitate was washed trice with cold water and twice with cold ether and allowed to dry under vacuum.

L1: Yield: 80%.[1]H NMR (500 MHz, DMSO-d6) δ (ppm): 1.94(s, 6H, –CH3); 2.69(s, 6H, –CH3); 7.73(dd, 2H, *J* = 6.4,3.4 Hz, Ar-H); 7.97 (dd, 2H, *J* = 6.4,3.5 Hz, Ar-H); 11.37 (s, 2H, -NOH). HRMS (ESI, positive mode) m/z for $[M+H]^+$ ion calculated: 402.0055, obtained: 402.004.

1.2.2. Synthesis of L3:

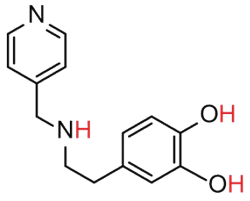

For the synthesis of L3 ligand, Dopamine hydrochloride (4.5 mM) was taken in 50ml ethanol: water (2:1 ratio) solution, followed by addition of Sodium Carbonate (9 mM). After Dopamine hydrochloride was completely soluble, 4-pyridine carboxaldehyde (4.5 mM) was added slowly into the solution. Then, the reaction mixture was stirred continuously for 2 hours at room temperature. White color precipitate appeared. The precipitate was filtered and washed thoroughly with water and ether, respectively and dried under air.

The white precipitate was dissolved in 30ml cold methanol under N2 atmosphere—thereby leading to white turbid solution. The whole reaction mixture was kept in an ice bath till the temperature came down to -5^0 C. Sodium Borohydride (1.5 mM) was very slowly added, and the reaction mixture was stirred for 2 hours. The yellow color complete clear solution appeared. Then, the reaction mixture was treated with dilute hydrochloric acid until the pH adjusted to 7. Then the mixture was evaporated and dried under vacuum.

L3: Yield: 80%. 1H NMR (500MHz, DMSO-d6) δ (ppm): 8.46(dd,2H, Ar-H); 7.26(dd,2H, Ar-H); 6.05(s, 1H, Ar-H); 5.59(dd,1H, Ar-H); 4.78(dd, 1H, Ar-H); 2.8 (t, 2H, NH-CH2-CH2); 2.6 (t,2H, Ar-CH2-CH2); 3.17(s,2H, Ar-CH2). HRMS (ESI, positive mode) m/z for $[M+H]^+$ ion calculated: 243.1128, obtained: 243.1128.

Synthesis of tyramine amine ligand(L4): L4 was prepared according to the literature[2].

Synthesis of cobalt complex(C1): Complex C1 was prepared according to the literature[3].

Synthesis of cobalt complex (C2):

L1 core (0.001 mol) was dissolved in 15 ml ethanol, then pyridine (0.0011 mol) was slowly added to stirring solution of the Copdd complex. Allow this solution to stir for 10 hours. After the addition of pyridine, the color of the solution turned brown from green. The precipitate will form in the reaction mixture. Filter the brown color precipitate formed and wash this precipitate with cold diethyl ether, and dry under vacuum.

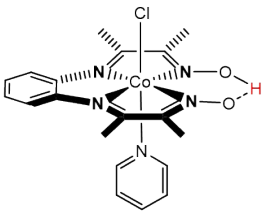

C2: Yield: 56%.[1]H NMR (500 MHz, D2O) δ (ppm): 2.33(s, 6H, –CH3); 2.52(s, 6H, –CH3); 7.25-7.29 (m,1H, Ar-H); 7.77 (tt, *J* = 7.7 Hz, 1H, Ar-H); 7.88-8.04 (m, 4H, Ar-H); 8.54 (tt, *J*= 8 Hz, 1H, Ar-H); 8.69-8.73 (m, 2H, Ar-H). HRMS (ESI, positive mode) m/z for $[C_{19}H_{21}Cl_2CoN_5O_2]^+$: Calculated: 480.0488; Experimental: 480.03667.

Synthesis of C3:

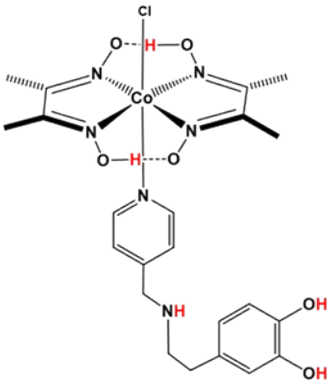

For the synthesis of C3, CodmgCl_2 was taken in a 10 ml dry methanol solution. Then L3 ligand was added slowly. The reaction mixture was refluxed for 3 hours. Then the solution was left for one day in the freeze. Brown color precipitate appeared. The precipitate was filtered and washed with dry ether and dried under a vacuum.

C3: Yield:64%. 1H NMR (500MHz, DMSO-d6) δ (ppm): 18.75 (s, 2H, H-bonded oxime); 10.14 (s, 1H, -NH); 9.3-9.6(s, 2H,-2OH); 8.43(d,2H,Ar-H); 7.77(d,2H,Ar-H); 6.94(s,1H,Ar-H); 6.33(s,1H,Ar-H); 5.94(s,1H,Ar-H);3.54(s,1H,-NH); 3.49(s,2H,-CH_2); 3.3-3.2(t,2H,-CH_2); 3.2-2.9(t,2H,-CH_2); 2.84 (s, 12H, 4CH_3). HRMS (ESI, positive mode): m/z for [$C_{22}H_{30}ClCoN_6O_6$]+: Calculated: 567.1163; Experimental: 567.1164.

Synthesis of C4:

For the synthesis of C4, we followed the same synthetic procedure as of C3. Here we used L4 ligand instead of L3. Brown color precipitate came. It was washed with methanol and ether respectively and dried under vacuum.

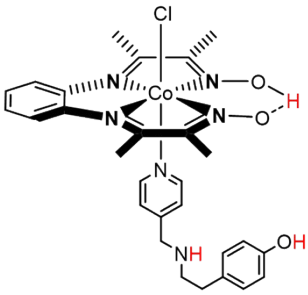

C4: Yield:73%. 1H NMR (500MHz, dmso-d6) δ (ppm): 18.45 (s, 1H, H-bonded oxime); 9.32(dd,2H, Ar-H); 8.83(dd,2H, Ar-H); 8.09(dd,2H, Ar-H); 7.53(dd,2H, Ar-H); 7.01(dd,2H, Ar-H); 6.69(d,2H, Ar-H); 3.40(s,2H,-CH_2); 3.21-3.07(t,2H,-CH_2); 2.79-2.71(t,2H,-CH_2); 2.33 (s, 12H, 4CH_3). HRMS (ESI, positive mode): m/z for [$C_{28}H_{33}N_6O_4Cl$] $^+$: Calculated: 613.0707; Experimental: 613.0576.

Supplementary Figures:

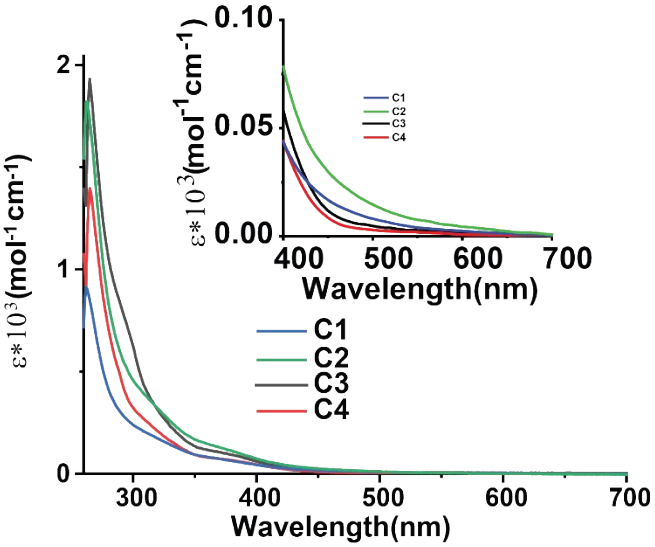

Figure S1. Optical spectra of C1-C4 recorded in a DMF medium at room temperature (blue trace **C1**, orange trace **C2**, black trace **C3**, red trace **C4**). The *d-d* transitions are shown in the inset.

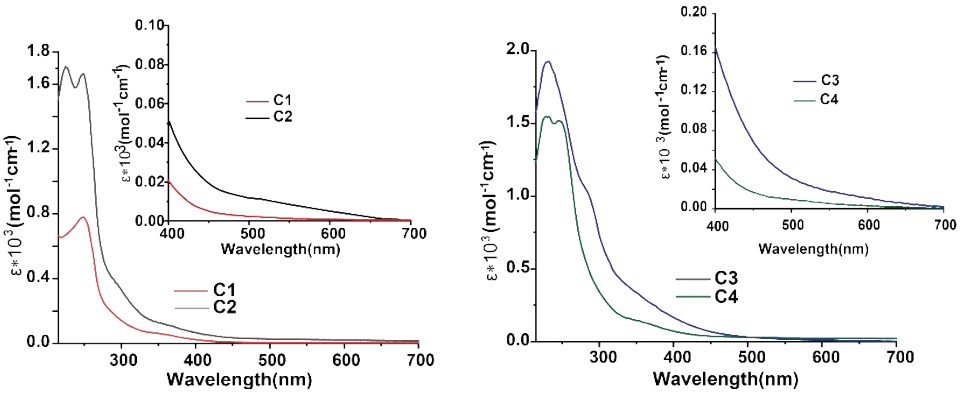

Figure S2. Optical spectra of **C1-C4** recorded in an aqueous solution at room temperature. The *d-d* transitions are shown in inset.

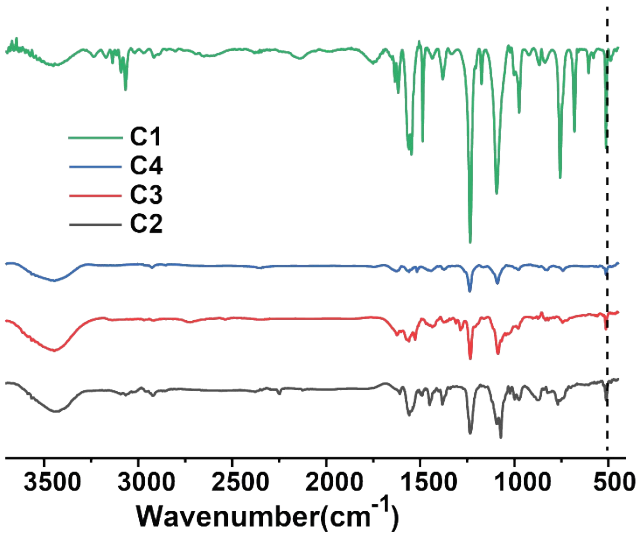

Figure S3. The comparative FTIR spectra of **C1-C4** complexes using KBr pellet at room temperature within scanning range 400 to 4000 cm^{-1}.

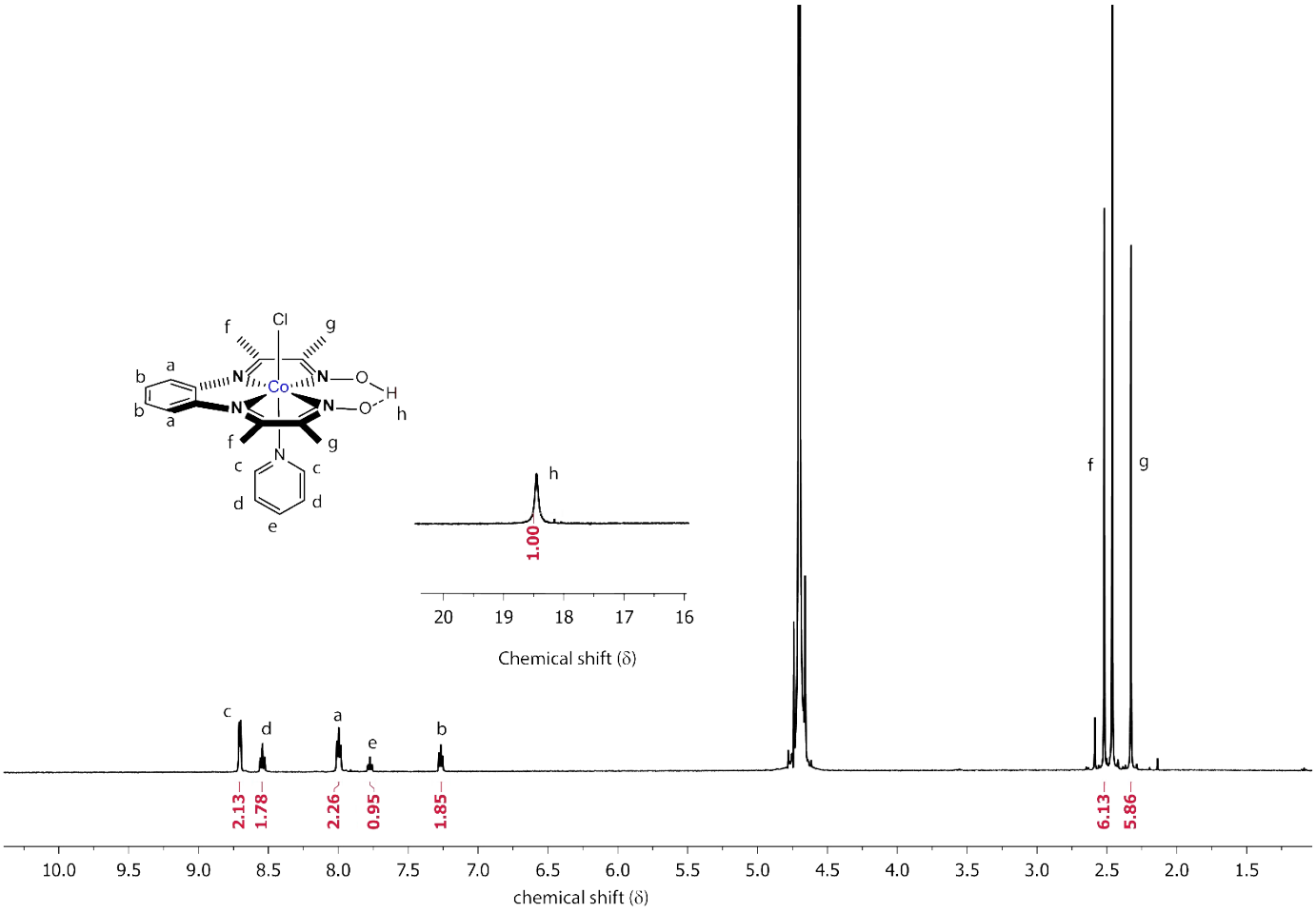

Figure S4. ^{1}H NMR spectrum of **C2** recorded in D_2O. Oxime peak recorded in dmso-d^{6} is shown in the inset.

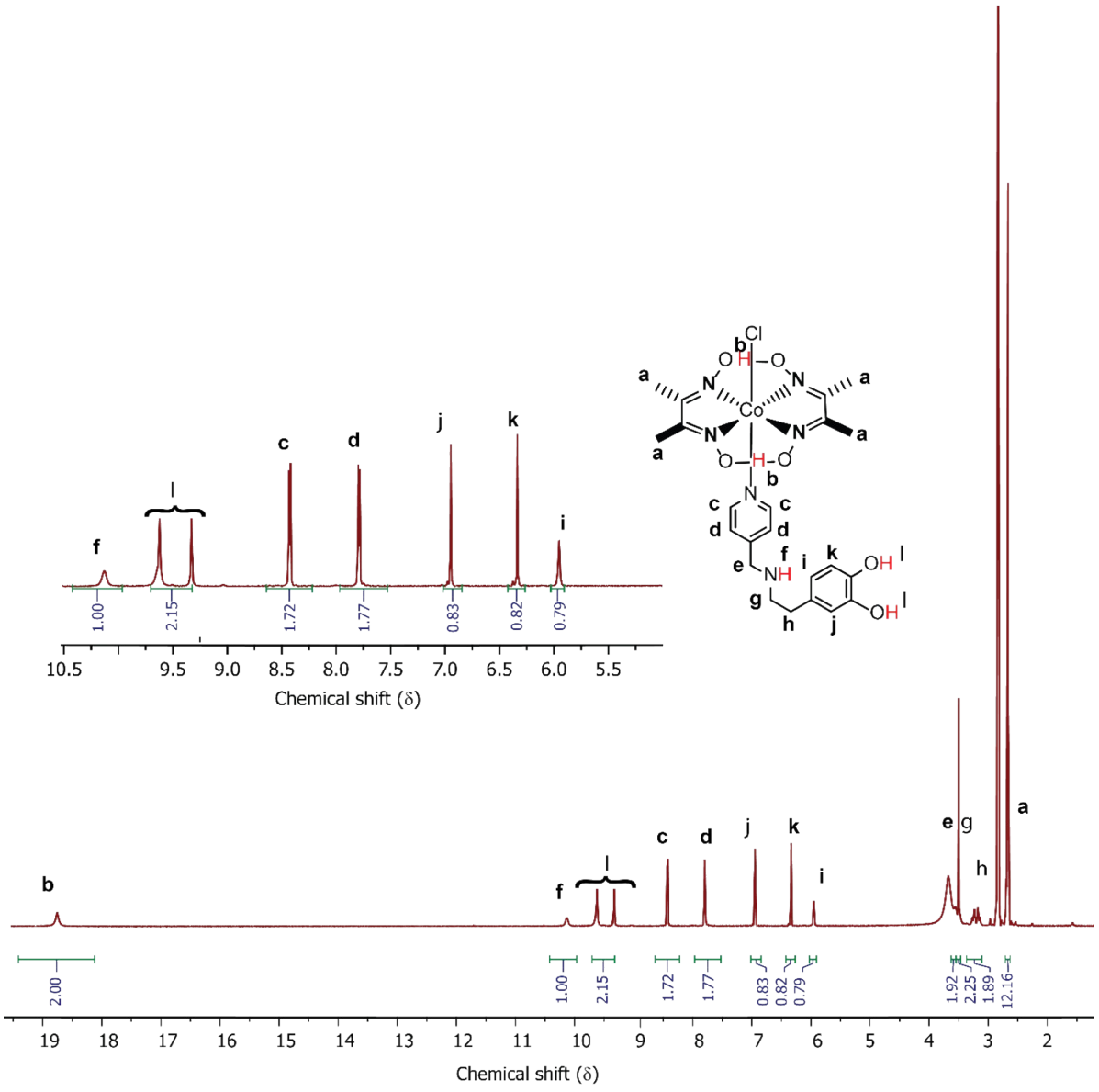

Figure S5. ^{1}H NMR spectrum of **C3** recorded in d^{6}-DMSO showing the peak for H-bonded oxime peak at 18.8 ppm.

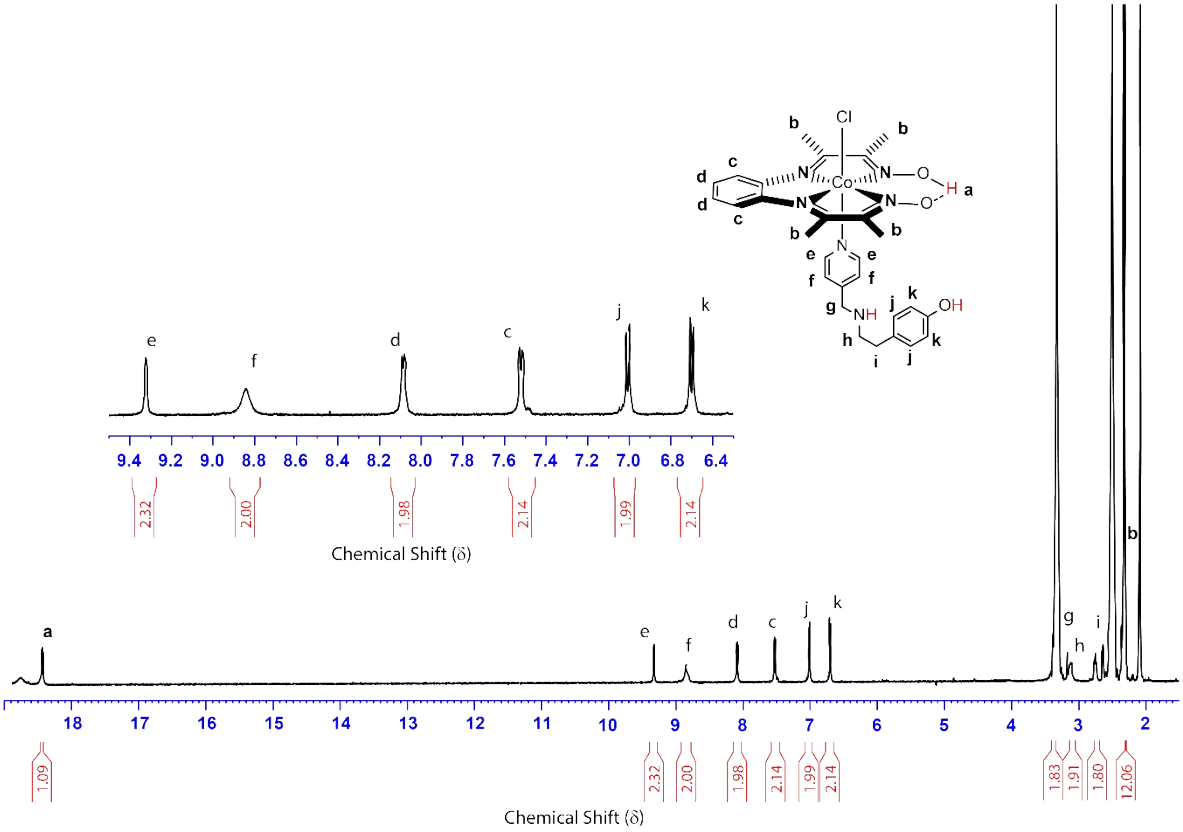

Figure S6.[1]H NMR spectrum of **C4** recorded in d[6]-DMSO showing the peak for H-bonded oxime peak at 18.8 ppm.

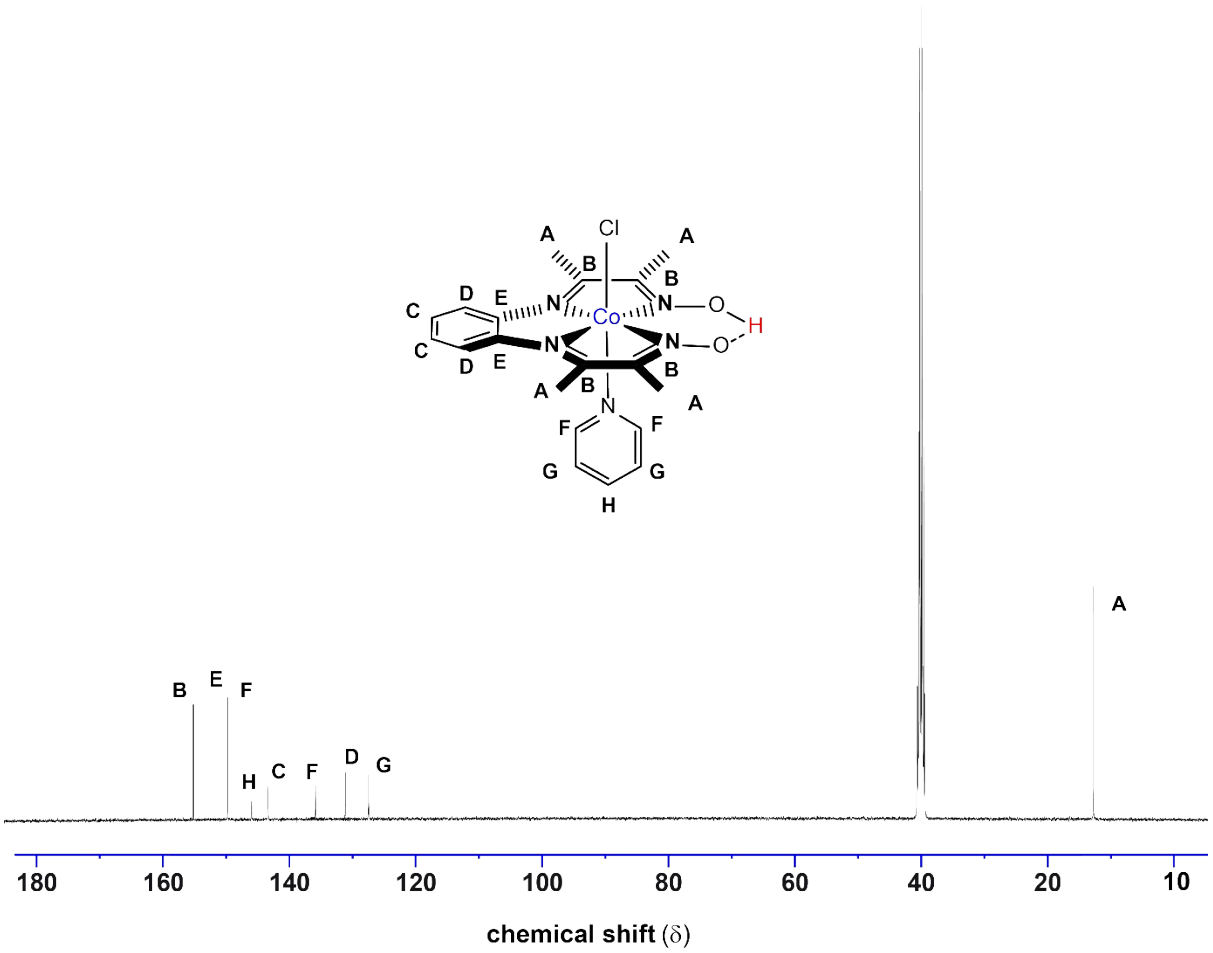

Figure S7. ^{13}C NMR spectrum of **C2** recorded in d^6-DMSO.

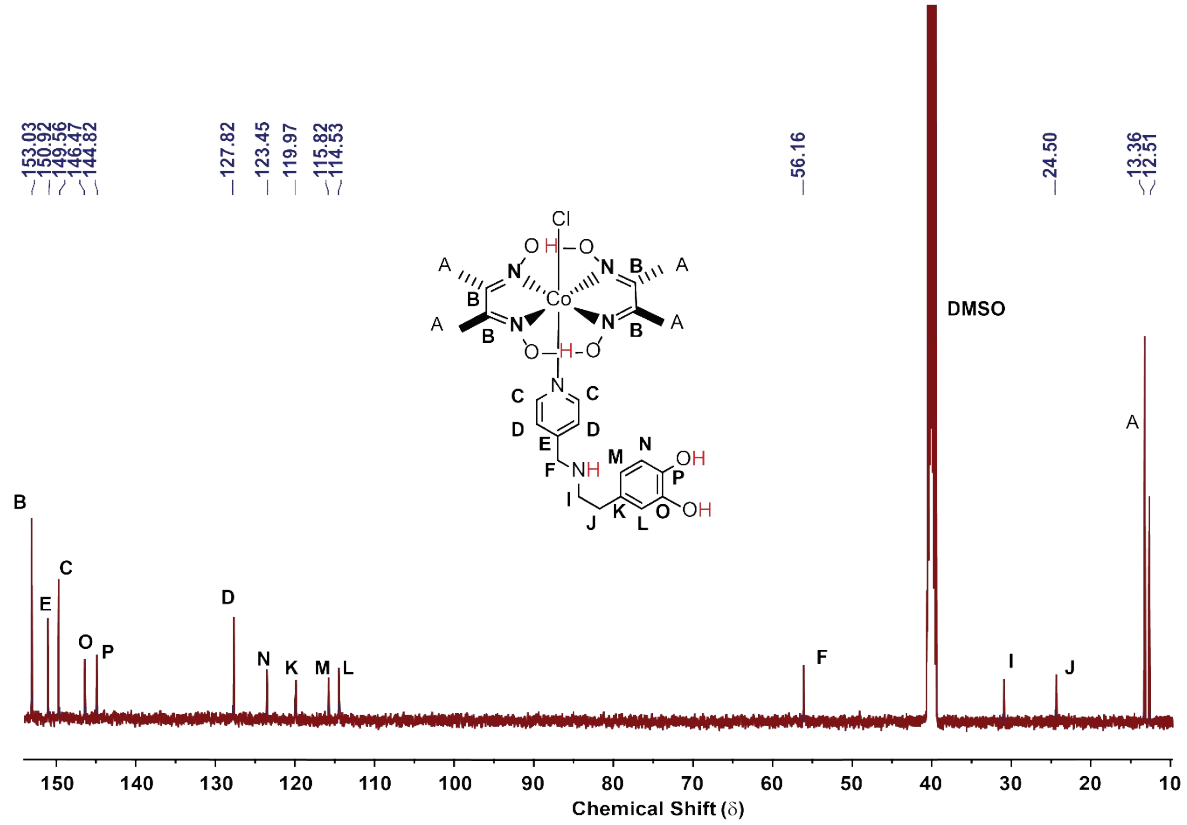

Figure S8. ^{13}C NMR spectrum of **C3** recorded in d^6-DMSO.

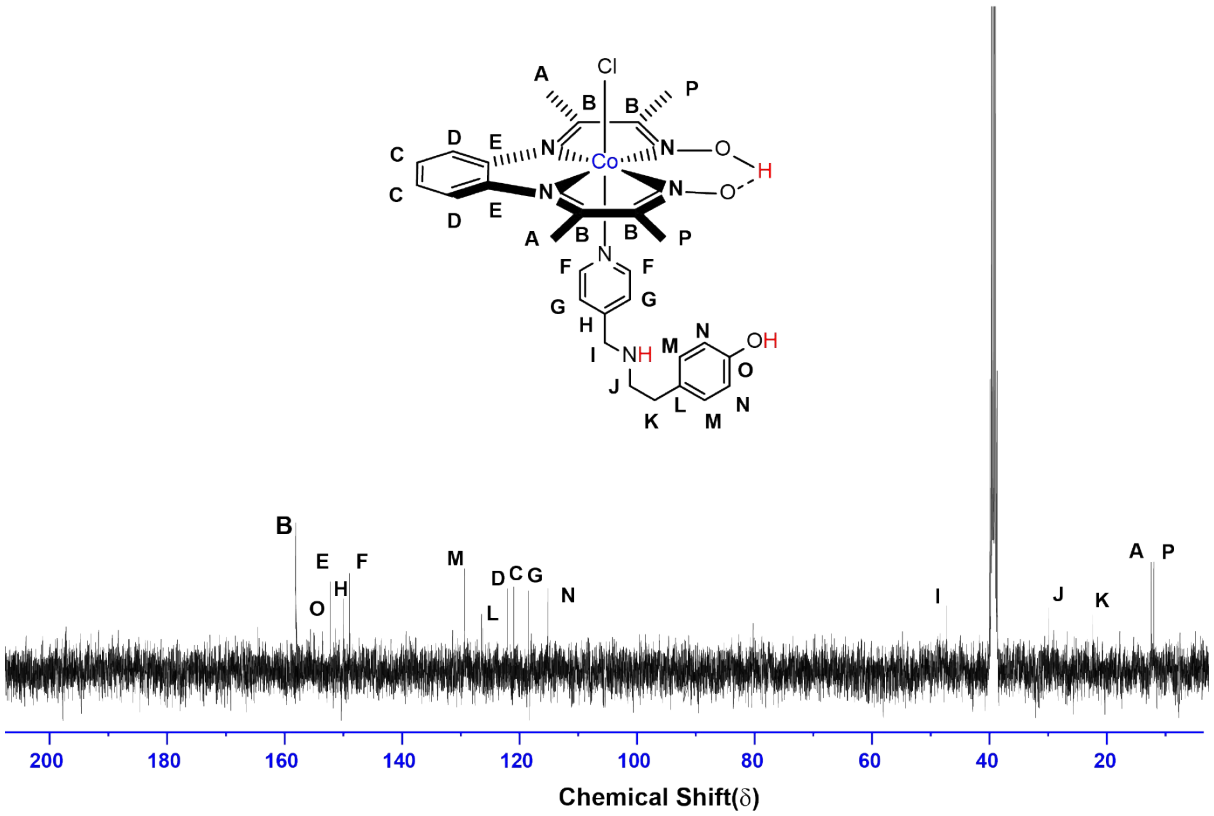

Figure S9. ^{13}C NMR spectrum of **C4** recorded in d^{6}-DMSO.

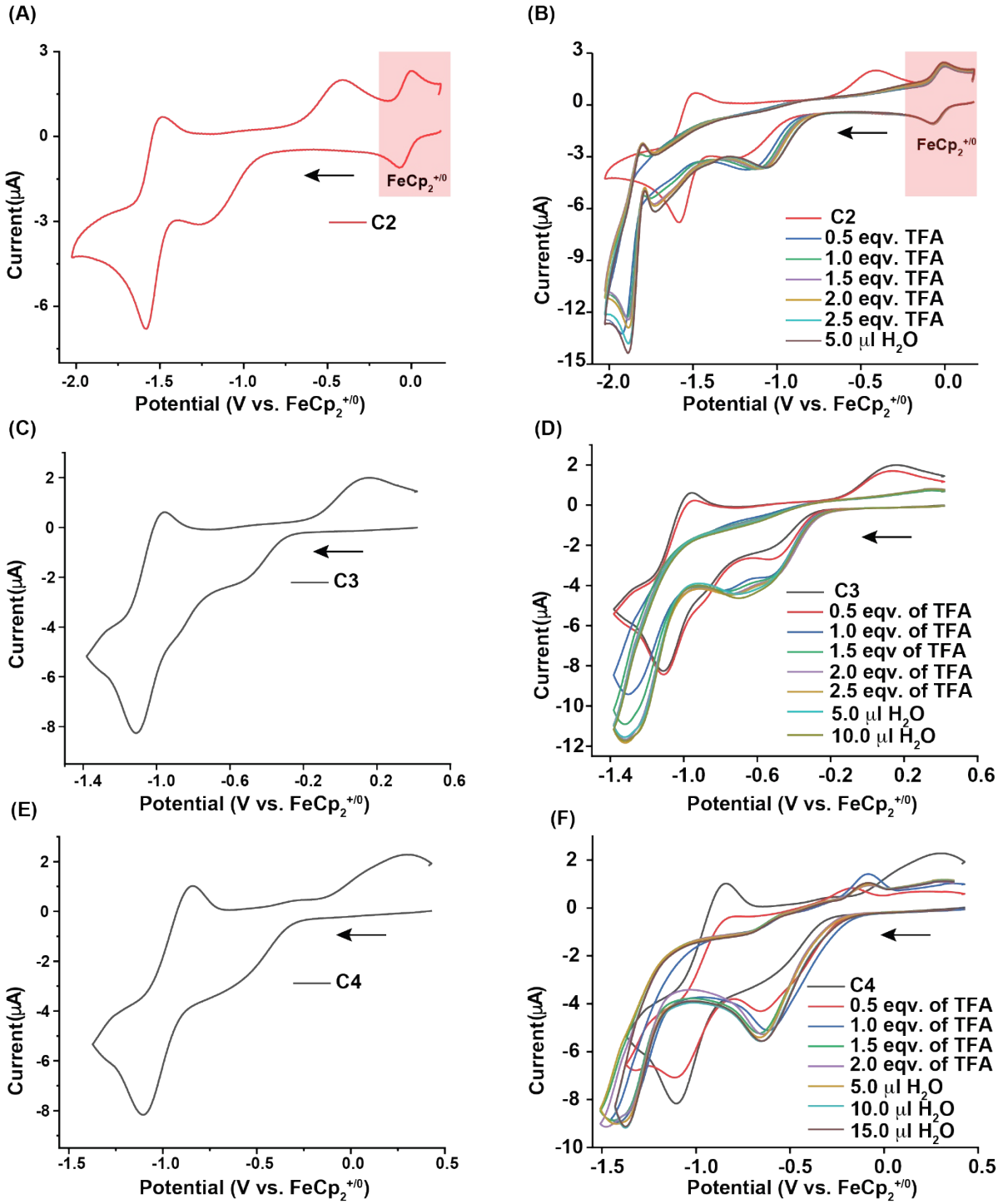

Figure S10. The comparative cyclic voltammograms (CVs) of **C2-C4** in DMF medium (A, C, and E) followed by the serial addition of Trifluoroacetic acid (TFA) and water (B, D, and F). Here glassy carbon disc working electrode, Ag/AgCl reference electrode, Pt-wire counter electrode was used along with TBAF as supporting electrolyte. The scan rate for each complex at different acid concentration is 1V/s. The initial scan direction is displayed by the black arrows.

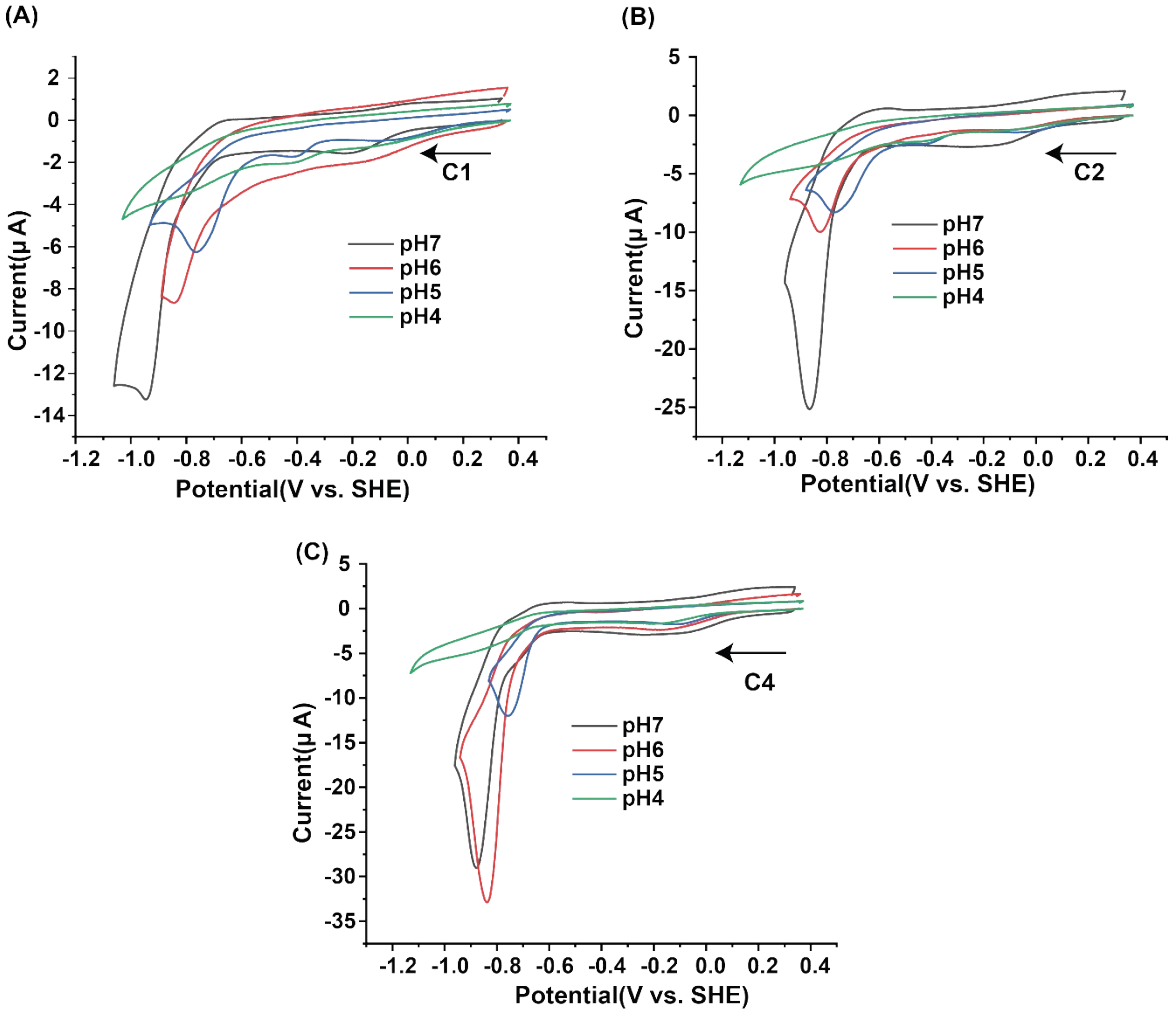

Figure S11. Cyclic voltammetry of **(A-D) C1-C4** in different pH solutions ranging from pH 4-pH 7 under Ar atmosphere at different scan rates. The scan rate for each pH for each complex indicates the current independent region. Utilized electrodes: working electrode-glassy carbon disc 1 mm diameter, reference electrode- Ag/AgCl, and counter electrode- platinum wire. pH7(black), pH6(red), pH5(blue), pH4(green) are shown in the figure.

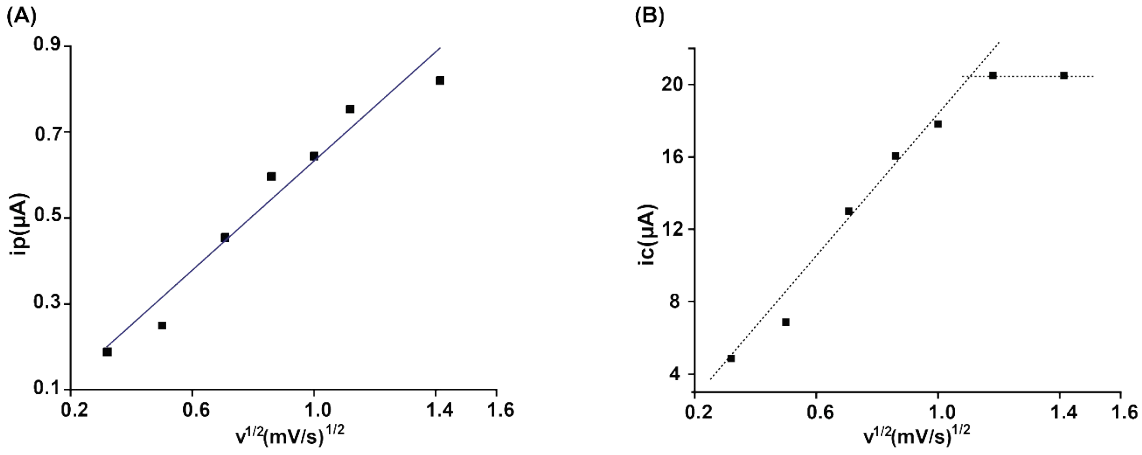

Figure S12. (A) Plot of i_p vs. square root of scan rate recorded for **C2**. The linear increase in the current with scan rate shows the stoichiometric nature of the signal. **(B)** Plot of i_c vs. square root of scan rate recorded for **C2**. The non-linear variation at higher scan rate indicates the involvement of catalysis.

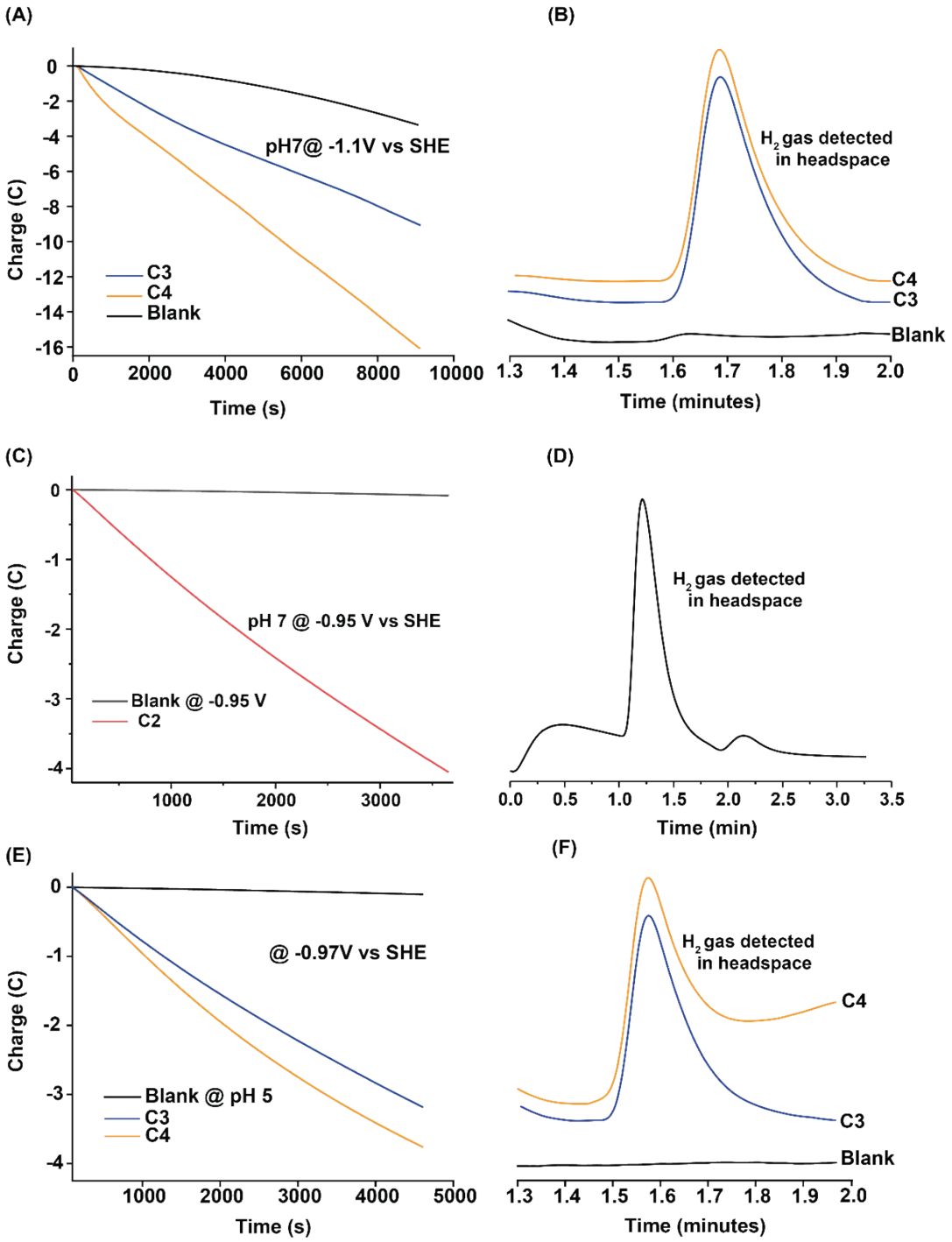

Figure S13. Bulk electrolysis data of complexes **C1-C4**, concentration 0.25mM using plastic chip electrode (2.5 cm x 2 cm) as working electrode, Ag/AgCl (3 M KCl) as reference electrode and coiled Pt-wire as counter electrode. (A) recorded at pH 7.0 at -1.1V vs. SHE for **C3** and **C4**; (C) at pH7.0 at -0.95V vs. SHE for complex **C2**; (E) at pH5.0 at -0.97V vs. SHE for **C3** and **C4**. (B), (D) and (F) represent corresponding GC data recorded after injecting 0.3ml of headspace gas using leur-lock gas-tight syringe at an interval of 1 hour. Blank (black trace), **C2** (red), **C3** (blue trace), **C4** (yellow trace) are shown in the figure.

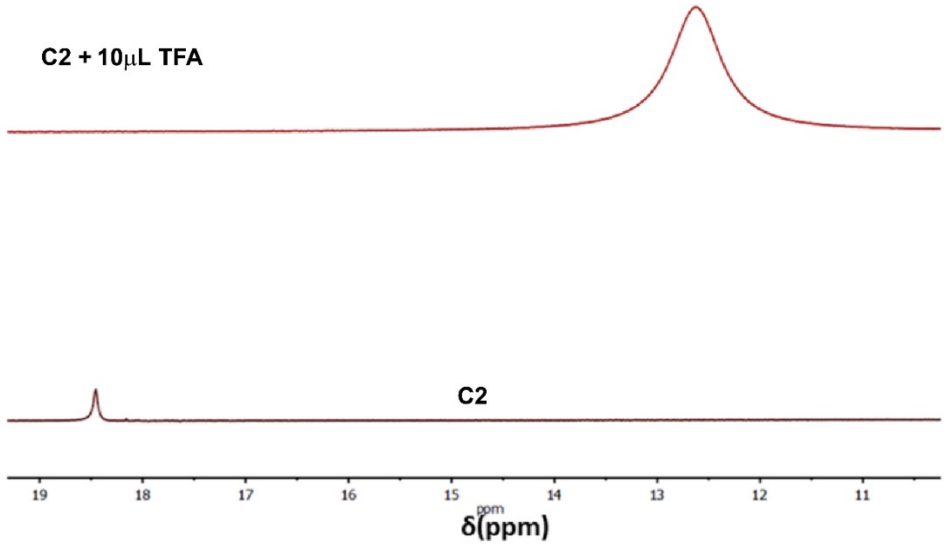

Figure S14. ^{1}H NMR of **C2** recorded in dmso-d^{6} in the region 10-19 ppm before (below) and after the addition of trifluoroacetic acid (TFA). The hydrogen-bonded oxime peak disappears in the presence of acid.

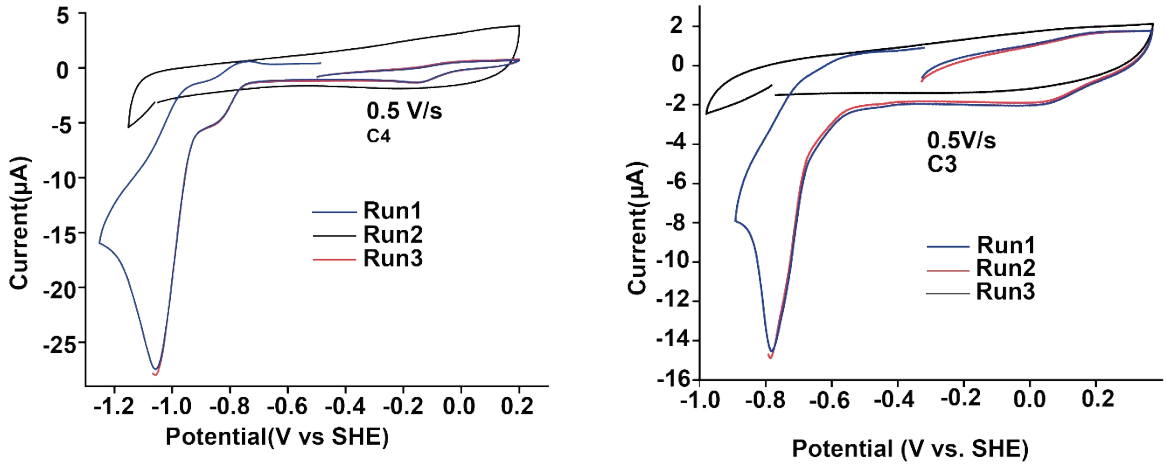

Figure S15. Rinse test of complexes **C3-C4** at 0.5 V/s. Three independent CV runs were recorded. A complete CV was carried out in the corresponding buffer medium in the first run. Then the working electrode was thoroughly rinsed with water and polished with alumina powder. The second run was stopped until the maximum current position observed. Then the working electrode was washed with only water, and the third run was executed in the blank buffer solution without complexity. No catalytic current was observed in the third run. This test proves that catalytic hydrogen production occurs via a homogeneous pathway.

Before Bulk Electrolysis

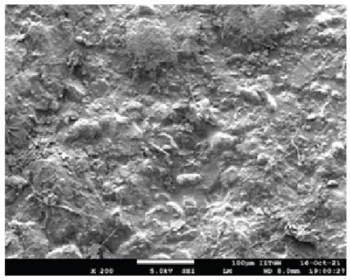

(A) FE-SEM

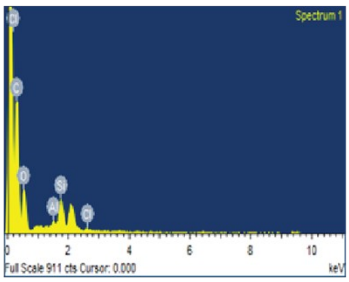

(B) EDS

Element	Weight %	Atomic %
C	66.03	73.48
O	28.90	24.15
Al	0.64	0.32
Si	3.90	1.86
Cl	0.53	0.20
Total	100	100

(C) EDS Analysis

After Bulk Electrolysis

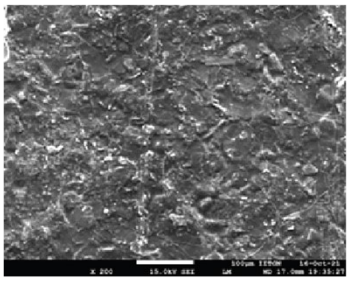

(D) FE-SEM

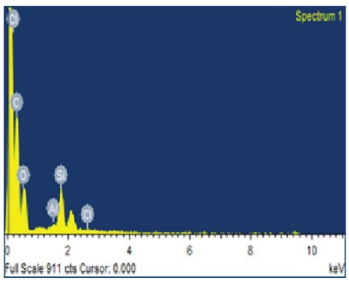

(E) EDS

Element	Weight %	Atomic %
C	63.00	70.87
O	31.20	26.35
Al	0.40	0.20
Si	5.29	2.55
Cl	0.10	0.04
Total	100	100

(F) EDS Analysis

Figure S16. SEM figure and EDX spectra of the plastic chip working electrode before and after the bulk electrolysis of **C3**. No detectable amount of cobalt deposition was observed on the material during electrolysis.

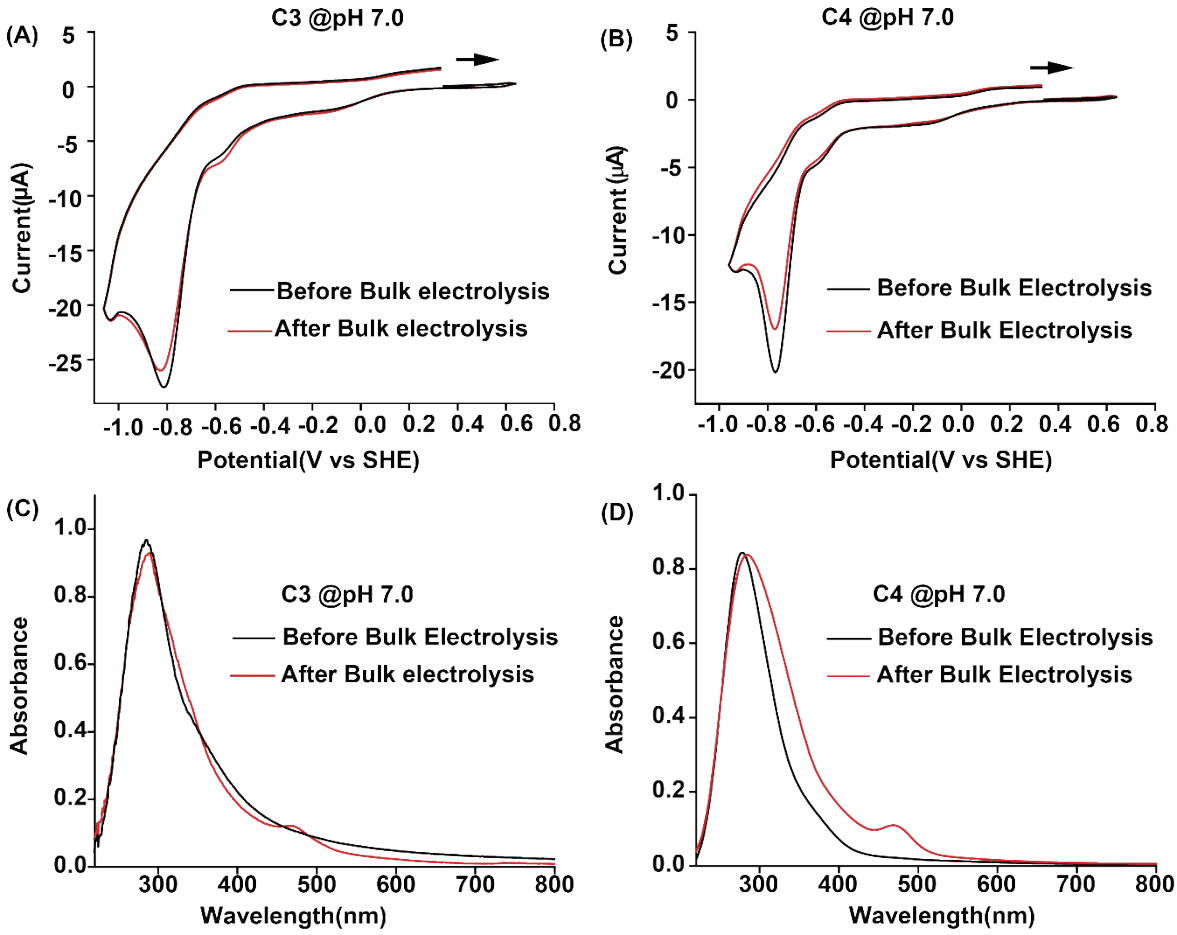

Figure S17. The comparative cyclic voltammetry (CV) data of **(A) C3** and **(B) C4** before (black trace) and after (red trace) following bulk electrolysis. The optical spectra recorded for **(C) C3** and **(D) C4** before (black trace) and after (red trace) following bulk electrolysis, the formation of Co(II) state is evident with the appearance of 470 nm band. All the data recorded at 298 K.

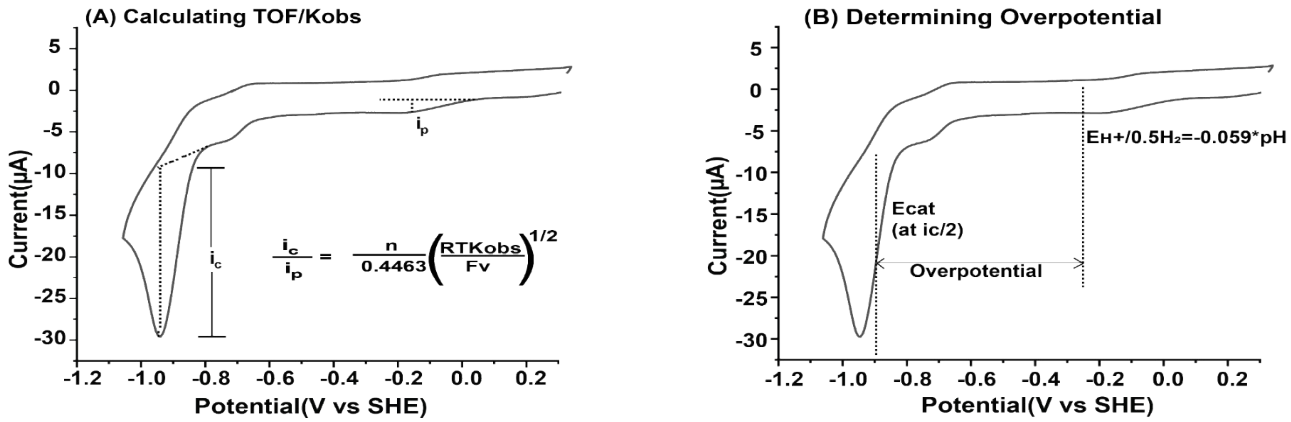

Figure S18. The representative cyclic voltammogram (CV) for the estimation of (**A**) stoichiometric (i_p) and catalytic current (i_c), along with (**B**) overpotential requirement (OP).

Table S1. Optical features of C1-C4 in DMF and water media

complex	Medium	**π- π*** **λ_{max}/nm** ($\varepsilon \times 10^3$/ $M^{-1}cm^{-1}$)	LMCT **λ_{max}/nm** (ε /$M^{-1}cm^{-1}$)	*d-d* **λ_{max}/nm** (ε /$M^{-1}cm^{-1}$)
C1	DMF	264(770)	316(185) 378(068)	520(10)
	H_2O	249(760)	289(160) 353(060)	512(10)
C2	DMF	262(1600)	314(371) 372(130)	560(17)
	H_2O	246(1600)	299(350) 366(110)	538(18)
C3	DMF	268(1600)	293(870) 379(900)	550(20)
	H_2O	230(1920)	291(90) 380(20)	518(18)
C4	DMF	270(1096)	317216) 378(068)	535(16)
	H_2O	246(1510)	358.7(139)	512(17)

Table S2. Stoichiometric redox potential of Co(III/II) and half-wave potential for Co(I) centric HER

pH	C1		C2		C3		C4	
	$-E_{Co^{III/II}}$ (V)	$-E_{cat/2}$(mV) [Co(I) centric]	$-E_{Co^{III/II}}$ (V)	$-E_{cat/2}$ (mV) [Co(I) centric]	$-E_{Co^{III/II}}$ (V)	$-E_{cat/2}$ (mV) [Co(I) centric]	$-E_{Co^{III/II}}$ (V)	$-E_{cat/2}$ (mV) [Co(I) centric]
7	0.234	887	0.156	812	0.189	880	0.176	814
6	0.133	765	0.146	757	0.186	784	0.180	781
5	0.064	670	0.048	670	0.170	722	0.103	693
4	0.109	700	0.123	739	0.121	692	0.185	741

Table S3. Electrocatalytic and photocatalytic H_2 production parameters for C1-C4 complexes in variable pH conditions

Complex	Electrocatalytic	Photocatalytic at pH 7.0

	pH 7.0		pH 6.0		pH 5.0		pH 4.0		TON (vs. catalyst)
	$TOF_{(s^{-1})}$	OP (Mv)	$TOF_{(s^{-1})}$	OP (Mv)	$TOF_{(s^{-1})}$	OP (Mv)	$TOF_{(s^{-1})}$	OP (Mv)	
C1	900 ± 10	477 ± 20	690 ± 15	420 ± 25	455 ± 12	375 ± 18	150 ± 10	534 ± 24	33 ± 5
C2	2500 ± 10	392 ± 18	690 ± 13	404 ± 20	300 ± 14	377 ± 17	340 ± 10	330 ± 19	62 ± 3
C3	6370 ± 5	467 ± 20	8400 ± 8	429 ± 16	1800 ± 10	425 ± 18	90 ± 11	449 ± 17	245 ± 4
C4	3716 ± 10	405 ± 21	7100 ± 12	434 ± 17	862 ± 5	397 ± 19	93 ± 8	514 ± 18	177 ± 5

Complex / **pH**	**C2**	**C3**	**C4**
	E^o(bulk electrolysis)	E^o (bulk electrolysis)	E^o(bulk electrolysis)
pH 7.0	-0.95	-1.1	-1.1
pH 5.0	n.r.	-0.97	-0.97
Faradaic Efficiency (%)	61±5 (pH 7.0)	95±5 (pH 7.0) 84±5 (pH 5.0)	67±5 (pH 7.0) 90±5 (pH 5.0)

Complex / **pH**	**C2**	**C3**	**C4**
	TON	TON	TON
pH 7.0	4.09±0.50	26.45±1.50	16.61±1.50
pH 6.0	n.r	125±5.00	92±5.00
pH 5.0	n.r	24.75±1.50	8.77±0.50

Table S4. Bulk electrolysis parameters for complexes C1-C4

Table S5. Comparative TON data from bulk electrolysis data

Experiment time: 2 hours; n.r. not recorded

Table S6. Comparative catalytic data of contemporary cobalt-based catalysts with C1-C4

Sr. No	**Molecular Cobalt catalyst**	**Electrocatalytic HER**		**Photocatalytic HER**	***Ref***
		TOF **(s^{-1})**	***OP*** **(mV)**	***TON***	
1	*Ht-CoM61A*	-	830	-	[4]
2	*Co (Iminopyridine)*	2.20 h^{-1}	450	-	[5]
3	*CoGGH*	-	600	2200	[6,7]

4	*$Co(DmgBF_2)_2(CH_3CN)_2$*	-	442	-	[8]
5	*$Co(dmg)_2$(4-pyridine tyrosine)Cl*	8830	507	-	[2]
6	*Co-salen tyrosine*	190	775	-	[9]
7	*$Co(dmg)_2$(4-ethylamine pyridine)Cl*	3800	457	-	[10]
8	*CoMP11-Ac*	-	852	905	[11]
9	*CoMC6*a*	680	-	10400	[12,13]
10	*(1- Iaa)$Co(dmg)_2$Cl*	3280	454	9200	[14]
11	*(4-Iaa)$Co(dmg)_2$Cl*	4925	428		
12	*(Histidine)$Co(dmg)_2$Cl*	4525	477	12180	
13	$Co(dmg)_2Cl\text{-}PO_3H$	1370	373		[15]
14	**C1**	**900**	**475**	21	[2,3]
15	**C2**	**2500**	**390**	42	**This work**
16	**C3**	**8400**	**465**	330	**This work**
17	**C4**	**7100**	**405**	280	**This work**

References:

(1) Perween, M.; Parmar, D. B.; Bhadu, G. R.; Srivastava, D. N. Polymer–Graphite Composite: A Versatile Use and Throw Plastic Chip Electrode. *Analyst* **2014**, *139* (22), 5919–5926. https://doi.org/10.1039/C4AN01405G.

(2) Dolui, D.; Khandelwal, S.; Shaik, A.; Gaat, D.; Thiruvenkatam, V.; Dutta, A. Enzyme-Inspired Synthetic Proton Relays Generate Fast and Acid-Stable Cobalt-Based H2 Production Electrocatalysts. *ACS Catal.* **2019**, *9* (11), 10115–10125. https://doi.org/10.1021/acscatal.9b02953.

(3) Razavet, M.; Artero, V.; Fontecave, M. Proton Electroreduction Catalyzed by Cobaloximes: Functional Models for Hydrogenases. *Inorg. Chem.* **2005**, *44* (13), 4786–4795. https://doi.org/10.1021/ic050167z.

(4) Kandemir, B.; Chakraborty, S.; Guo, Y.; Bren, K. L. Semisynthetic and Biomolecular Hydrogen Evolution Catalysts. *Inorg. Chem.* **2016**, *55* (2), 467–477. https://doi.org/10.1021/acs.inorgchem.5b02054.

(5) Stubbert, B. D.; Peters, J. C.; Gray, H. B. Rapid Water Reduction to H2 Catalyzed by a Cobalt Bis(Iminopyridine) Complex. *J. Am. Chem. Soc.* **2011**, *133* (45), 18070–18073. https://doi.org/10.1021/ja2078015.

(6) Kleingardner, J. G.; Kandemir, B.; Bren, K. L. Hydrogen Evolution from Neutral Water under Aerobic Conditions Catalyzed by Cobalt Microperoxidase-11. *J. Am. Chem. Soc.* **2014**, *136* (1), 4–7. https://doi.org/10.1021/ja406818h.

(7) Chakraborty, S.; Edwards, E. H.; Kandemir, B.; Bren, K. L. Photochemical Hydrogen Evolution from Neutral Water with a Cobalt Metallopeptide Catalyst. *Inorg. Chem.* **2019**, *58* (24), 16402–16410. https://doi.org/10.1021/acs.inorgchem.9b02067.

(8) Berben, L. A.; Peters, J. C. Hydrogen Evolution by Cobalt Tetraimine Catalysts Adsorbed on Electrode Surfaces. *Chem. Commun.* **2010**, *46* (3), 398–400. https://doi.org/10.1039/B921559J.

(9) Khandelwal, S.; Zamader, A.; Nagayach, V.; Dolui, D.; Mir, A. Q.; Dutta, A. Inclusion of Peripheral Basic Groups Activates Dormant Cobalt-Based Molecular Complexes for Catalytic H2 Evolution in Water. *ACS Catal.* **2019**, *9* (3), 2334–2344. https://doi.org/10.1021/acscatal.8b04640.

(10) Dolui, D.; Mir, A. Q.; Dutta, A. Probing the Peripheral Role of Amines in Photo- and

Electrocatalytic H2 Production by Molecular Cobalt Complexes. *Chem. Commun.* **2020**, *56* (94), 14841–14844. https://doi.org/10.1039/D0CC05786J.
(11) Edwards, E. H.; Jelušić, J.; Chakraborty, S.; Bren, K. L. Photochemical Hydrogen Evolution from Cobalt Microperoxidase-11. *J. Inorg. Biochem.* **2021**, *217*, 111384. https://doi.org/10.1016/j.jinorgbio.2021.111384.
(12) Firpo, V.; Le, J. M.; Pavone, V.; Lombardi, A.; Bren, K. L. Hydrogen Evolution from Water Catalyzed by Cobalt-Mimochrome VI*a, a Synthetic Mini-Protein. *Chem. Sci.* **2018**, *9* (45), 8582–8589. https://doi.org/10.1039/C8SC01948G.
(13) Edwards, E. H.; Le, J. M.; Salamatian, A. A.; Peluso, N. L.; Leone, L.; Lombardi, A.; Bren, K. L. A Cobalt Mimochrome for Photochemical Hydrogen Evolution from Neutral Water. *J. Inorg. Biochem.* **2022**, *230*, 111753. https://doi.org/10.1016/j.jinorgbio.2022.111753.
(14) Dolui, D.; Das, S.; Bharti, J.; Kumar, S.; Kumar, P.; Dutta, A. Bio-Inspired Cobalt Catalyst Enables Natural-Sunlight-Driven Hydrogen Production from Aerobic Neutral Aqueous Solution. *Cell Rep. Phys. Sci.* **2020**, *1* (1), 100007. https://doi.org/10.1016/j.xcrp.2019.100007.
(15) Mir, A. Q.; Saha, S.; Mitra, S.; Guria, S.; Majumder, P.; Dolui, D.; Dutta, A. The Rational Inclusion of Vitamin B6 Boosts Artificial Cobalt Complex Catalyzed Green H2 Production. *Sustain. Energy Fuels* **2022**, *6* (18), 4160–4168. https://doi.org/10.1039/D2SE00734G.